Supporting Information

Overcoming the limitations of low-bandgap $Cu_2ZnSn(S,Se)_4$ devices under indoor light conditions: From design to prototype IoT application

Vijay C. Karade[1,2,†], Jihoo Lim[3,†], Kuldeep Singh Gour[1,2], Jun Sung Jang[1], So Jeong Shin[4], Jong H. Kim[4], Bum Seung Yang[5], Hyuntae Choi[6], Temujin Enkhbat[7], JunHo Kim[7], Jae Sung Yun[3,8], Hae Nam Jang[9], Jae Ho Yun[2], Jongsung Park[9,*], and Jin Hyeok Kim[1,*]

[1]Department of Materials Science and Engineering and Optoelectronics Convergence Research Center, Chonnam National University, Gwangju 61186, Republic of Korea.

[2]Department of Energy Engineering / KI for Energy Materials and Devices, Korea Institute of Energy Technology (KENTECH), 200 Hyeoksin-ro, Naju, Jeonnam 58330, Republic of Korea.

[3]Australian Centre for Advanced Photovoltaics (ACAP), School of Photovoltaic and Renewable Energy Engineering, University of New South Wales, Sydney, NSW 2052, Australia.

[4]Department of Molecular Science and Technology, Ajou University, Suwon, 16499, Republic of Korea.

[5]Powercons, Ltd., Naju, Joennam, 58324, Republic of Korea.

[6]Satellite Technology Research Center, Korea Advanced Institute of Science and Technology, Daejeon 34141, Republic of Korea.

[7] Department of Physics, Incheon National University, Incheon, 22012, Korea.

[8]Department of Electrical and Electronic Engineering, Advanced Technology Institute (ATI), University of Surrey, Guildford, Surrey GU2 7XH, United Kingdom.

[9]Department of Energy Engineering, Future Convergence Technology Research Institute, Gyeongsang National University, Jinju, 52849, Republic of Korea.

[†] VCK and JL equally contributed to this work

[*]Corresponding authors

Jongsung Park (Email: j.park@gnu.ac.kr)

Jin Hyeok Kim (Email: jinhyeok@chonnam.ac.kr)

1. Experimental details

1.1 Metallic precursor and $Cu_2ZnSn(S,Se)_4$ absorber thin film preparation

i) Initially, 2.5 × 2.5 cm^2 molybdenum (Mo) coated soda-lime glass (SLG) substrates were ultrasonically cleaned using isopropyl alcohol and deionized water (DI) for 10 min. sequentially and dried by an N_2 gun. The cleaned Mo substrates were further used to deposit the metal precursor layers. The precursor thin films with Cu/Sn/Zn/Mo stacking order were prepared via a direct current (DC) magnetron sputtering technique. Pure metallic targets Cu, Zn, and Sn with 99.999 % purity (TASCO, USA) of 3-inch size were used for the sputtering process. All the thin films, including the reference and double cation experiment, were fabricated together by DC sputtering at 8 mTorr with sputtering power of Cu: 0.68 W/cm^2 (2800) s, Sn: 0.68W/cm^2 (1800), and Zn: 0.68W/cm^2, (2000 s), respectively. The substrates were rotated at 5 rpm during the sputtering process.

ii) To incorporate Ge, first Ge was deposited Mo substrates before precursor deposition, whereas for Ag incorporation, the Ag was deposited over the precursor. The high-purity 3 mm Ag and Ge shots purchased from i-TASCO (USA) were used to deposit the Ag and Ge by thermal evaporation. For Ag and Ge, the deposition rate of 0.1 Å/s was kept. The total thickness of Ag and Ge was kept around 8-10 nm for both layers as optimized in our previous reports. [S1, S2]

iii) Further, to get the Cu-Zn and Cu-Sn alloys, the soft annealing process was employed on all the metallic precursors, where they were heated at 280 ℃ for 1 h in an Ar atmosphere in the tube furnace. The precursors were placed at the center of the tube, and before the soft-annealing process, the tube was purged with Ar gas three times. The ramping rate for the process was maintained up to 10 ℃/min. After the process, all the samples were allowed to cool down naturally to room temperature (RT).

iv) The soft-annealed precursor thin films were then annealed in a chalcogenide environment with mixed S and Se powder (0.2 g), with an S: Se ratio of 1:100. Before the rapid thermal annealing (RTA) process, the blank annealing process was performed at 600 ℃ for 15 min. with an empty graphite box to remove residual S and Se content. Then, all the samples were placed in a graphite box for the process, which was subsequently placed into a chamber-type RTA system. The chamber was evacuated to a base pressure of 1.0×10^{-5} Torr, and then the initial chamber pressure was controlled up to 500 Torr using Ar gas. After that, the chamber was heated at 540 ºC with a ramping rate of 10 ºC/s, and the temperature was maintained for 7.5 min. After the RTA process, the annealed thin films were naturally cooled to RT.

1.2 Device Fabrication process

The CZTSSe device was fabricated by depositing the multi-layered structure of Al/AZO/i-ZnO/CdS/CZTSSe/Mo/SLG. a) Initially, all the CZTSSe absorbers were etched with 0.2 M potassium cyanide at RT for 2 min., subsequently rinsed using DI water, and dried by an N_2 gun. b) A ~50 nm thick CdS buffer layer was deposited by the chemical bath deposition technique with a precursor of 0.0015 M $CdSO_4$, 2.871 M NH_3, and 0.05 M thiourea at 60 ºC for 14.5 min. and subsequently rinsed in DI water. c) The i-ZnO and Al-doped ZnO-based (AZO) transparent conducting oxide layer were prepared via the RF magnetron sputtering technique at RT and 350 ºC, respectively. The RF powers of 50 W and 70 W at a working pressure of 1 mTorr, under Ar and O_2 mixed plasma and just Ar plasma were used for i-ZnO and AZO deposition, respectively. The thickness of i-ZnO and AZO were maintained to 60 and 600 nm, respectively. d) Finally, a nearly 1 μm thick Al top grid was deposited using the DC sputtering technique with the area of the fabricated solar cells up to 0.3 cm^2. During light and IPV J-V measurements, no antireflecting coating was used over the cell.

1.3 Characterizations of the CZTSSe absorber thin films and solar cells

The phase purity and structural properties of thin films were measured by high-resolution XRD (X'pert PRO, Philips, Eindhoven, Netherlands) from 5° to 90° with a step size of 0.05 2θ. The thin film's surface morphology, cross section, and composition were characterized using field emission scanning electron microscopy (Gemini 500 + EDS (Oxford)). The device efficiency (PCE) and external quantum efficiency (EQE) spectra for solar cells were characterized by a class AAA solar simulator (WXS-155S-L2, WACOM, and Japan) with the condition of AM 1.5G, 100 mW/cm^2, and 25 ºC and QEX10 spectral response system (S-9230, SOMA Optics, Japan) respectively. The KPFM measurements were taken using an AFM (NX-10, Park Systems) in an ambient atmosphere. The data were collected using a 6-10 nm radius of curvature (HA_NC/Au, TipsNano) with a scan rate of 0.4 Hz and an AC voltage of −1 to +1 V. For the light conditions, WLED was used source for the illumination. Admittance spectroscopy (AS) was performed using an LCR meter (E4980A, Agilent) by applying an AC frequency of 2 Hz to 1 MHz to the solar cell device in the temperature range of 300–90 K. To analyze the AS results, we employed the Cp-D mode, which provides good accuracy in low-resistance conditions. The transmission electron microscopy (TEM) was obtained using a JEOL-3010 at an operating voltage of 100 kV using an FEI, Tecnai G2-F30. TEM samples were prepared by focus ion beam (FEI, Helios G3 CX) at an operating voltage of 30 kV onto Ni-TEM grids. An

impedance analyzer (Hewlett Packard, HP4284) is used to perform the C-V measurement. The capacitance (C) vs. voltage (V) plot of the devices was collected from -2.5 V to 1.0 V DC bias voltage at RT under dark conditions with 30 mV and 100 kHz AC signals. The elemental distribution profiles Ag and Ge doped in the CZTSSe absorber layer were determined by time-of-flight secondary ion mass spectroscopy (TOF-SIMS, (IONTOF, TOF.- SIMS5 - 100). The primary beam of Bi^+ ions at 30 keV and the current were 0.455 pA (±0.05pA) was used. Morever, the secondary sputtering beam of Cs^+ ions at 1 keV and the related current was approximately 65 nA (±5 nA). The area of the samples, 300 × 300 μm^2, was kept constant.

1.4 Low light intensity measurements

The present study performed the IPV *J-V* measurement only at 400-1200 lux, as indoor light is artificial light based on FL lamps or LEDs, which generally have ~1,000 times lower light (200-1,000 lux) intensities than outdoor sunlight; besides, the emission wavelength is limited to the visible light region (300-750 nm). Before starting the *J-V* measurement, the lamps were started and allowed to stabilize until they provided the characteristic spectrum. Then, indoor light J-V characteristics of CZTSSe solar cells were measured with Keithley 4200 source meter under illumination intensities of 400, 800, and 1200 lux using calibrated WLED and FL-4000K lamps. An FL-4000K lamp (OSRAM DULUXSTAR) and a WLED (LED 5w A60 Globe) were used as light sources for indoor lighting conditions. The spectrum of the indoor light source was collected using a lux meter, and the digital photographs of the measurement setup are given in **Figure S1.**

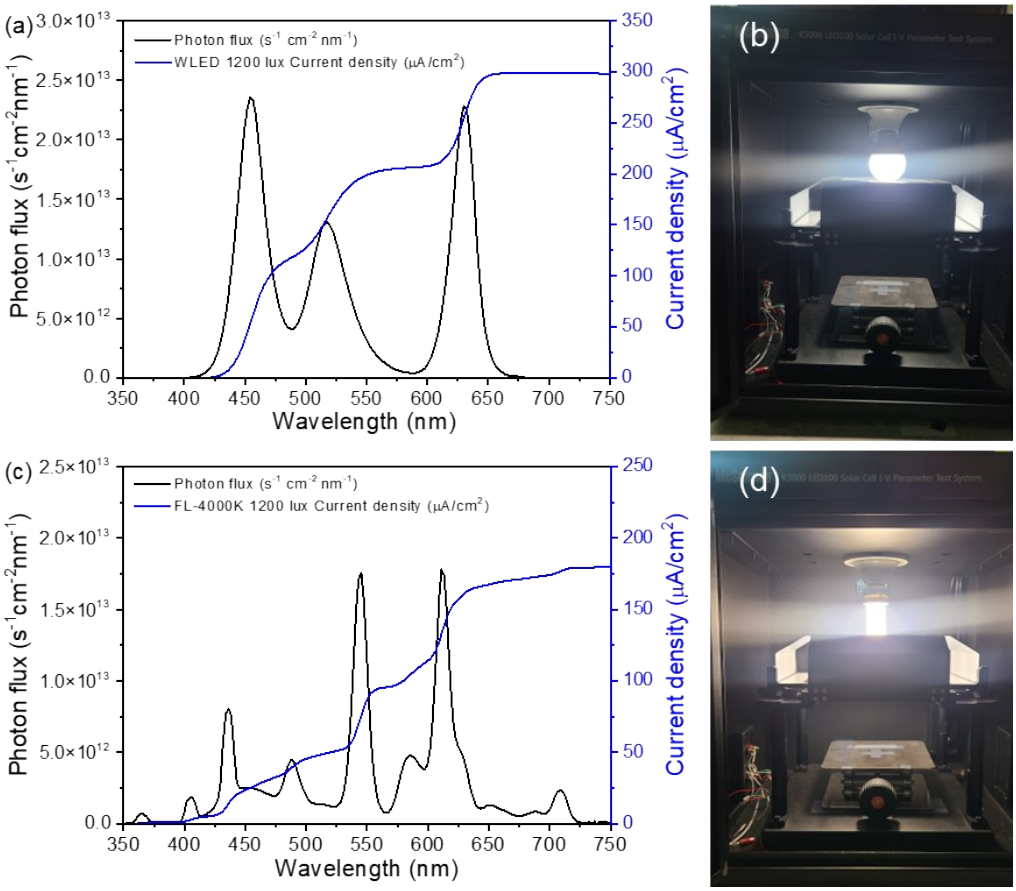

Figure S1. Photon flux spectrum at 1200 lux (a) WLED and (c) FL-4000K and corresponding digital photographs of measurement setup for (b) WLED and (d) FL-4000K light sources.

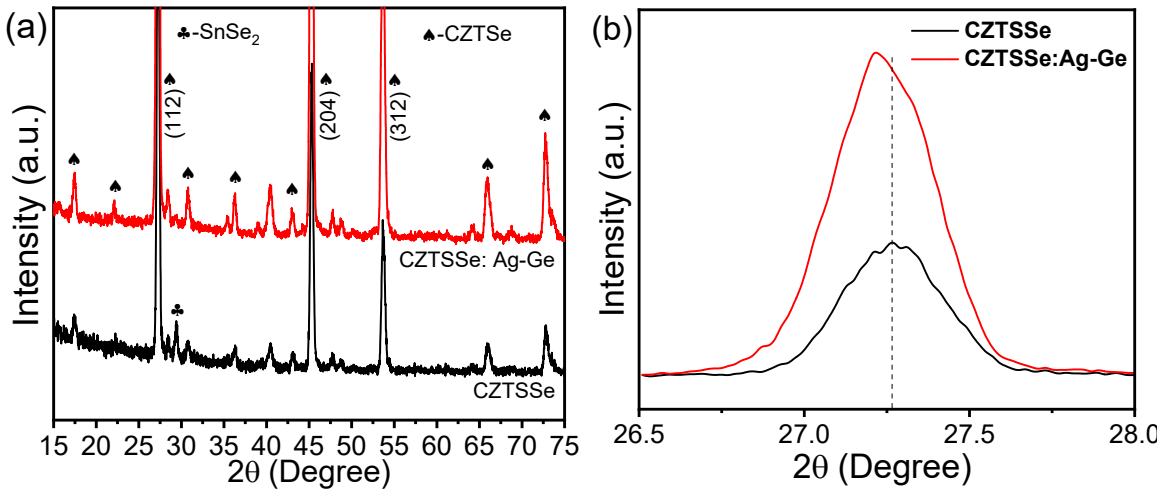

Figure S2. (a) X-ray diffraction (XRD) pattern and (b) shift in a characteristic peak position corresponding to (1 1 2) plane of the CZTSSe and CZTSSe:Ag-Ge thin films.

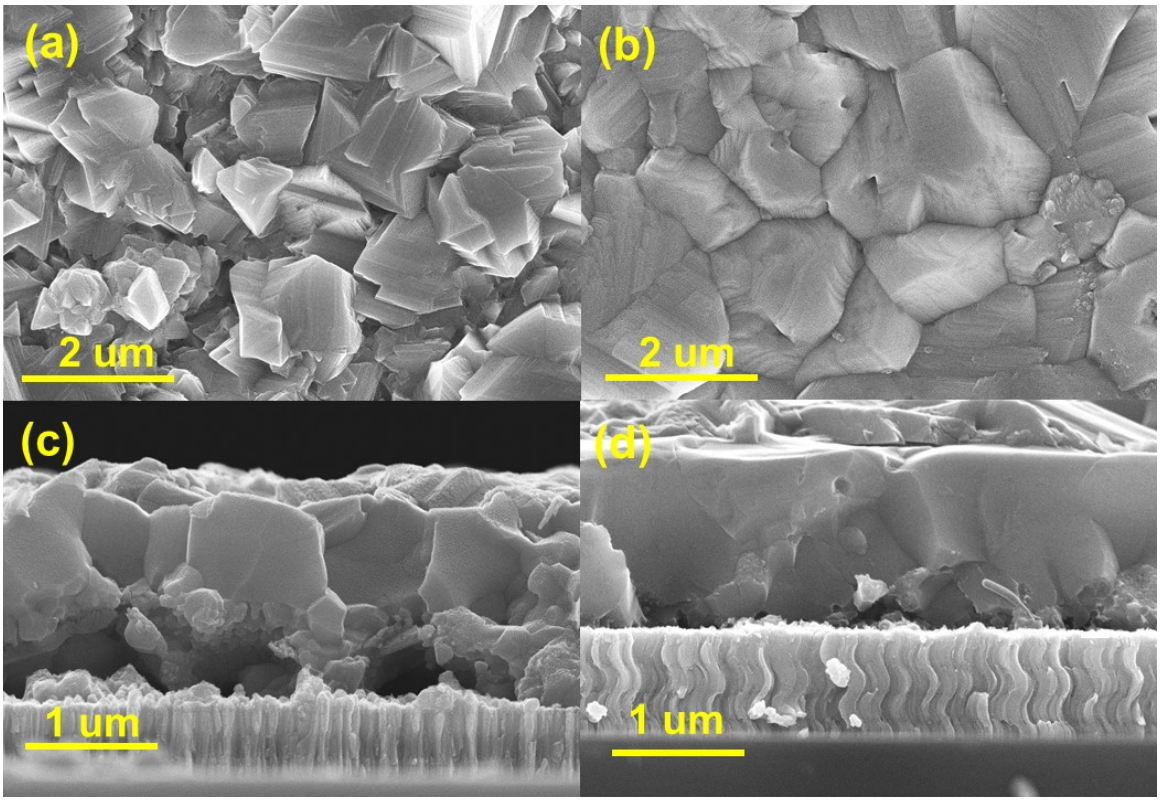

Figure S3. Field emission scanning electron microscope (FE-SEM) surface and cross-sectional images of the CZTSSe and CZTSSe: Ag-Ge thin films.

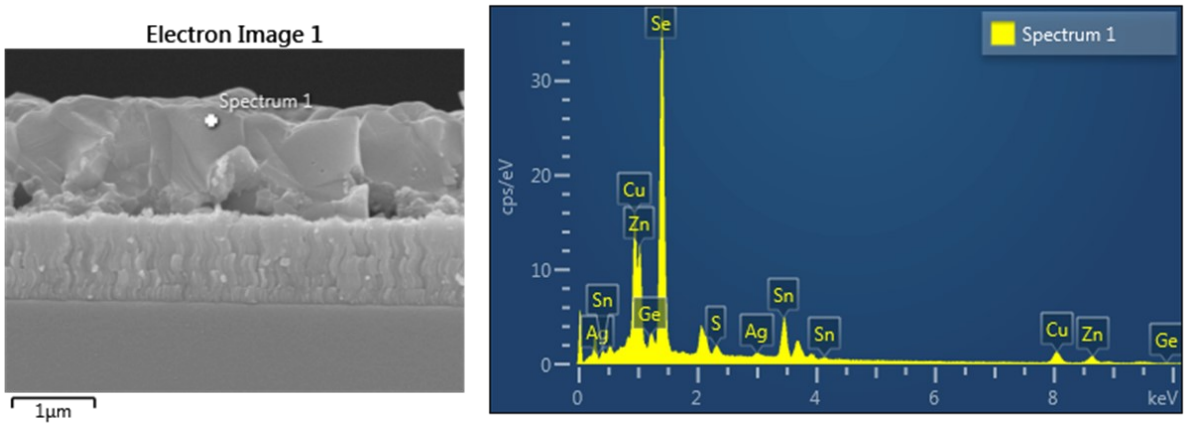

Figure S4. Cross-sectional FE-SEM image of the CZTSSe:Ag-Ge thin film and corresponding EDS spectra.

Table S1. The EDS data obtained from the FE-SEM image of the CZTSSe:Ag-Ge thin film.

Element	Line Type	Apparent Concentration	Wt %	At %	Standard Label
S	K series	1.57	1.08	2.56	FeS2
Cu	L series	21.11	18.44	22.06	Cu
Zn	L series	12.51	14.96	17.40	Zn
Ge	L series	0.05	0.059	0.06	Ge
Se	L series	46.73	49.39	47.56	Se
Ag	L series	1.27	0.95	0.67	Ag
Sn	L series	20.78	15.13	9.69	Sn
Total			100.00	100.00	

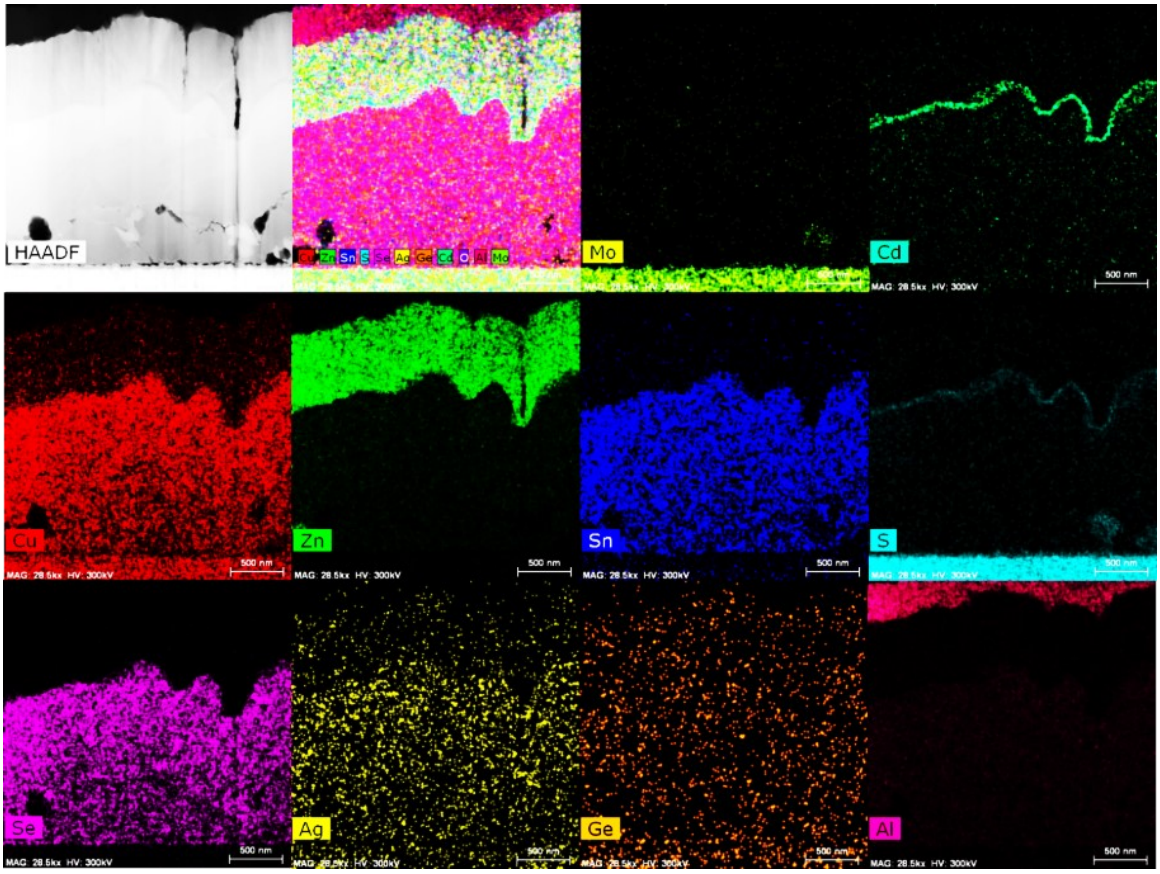

Figure S5. Cross-sectional HAADF-STEM image and EDS mapping of the CZTSSe: Ag-Ge solar cell.

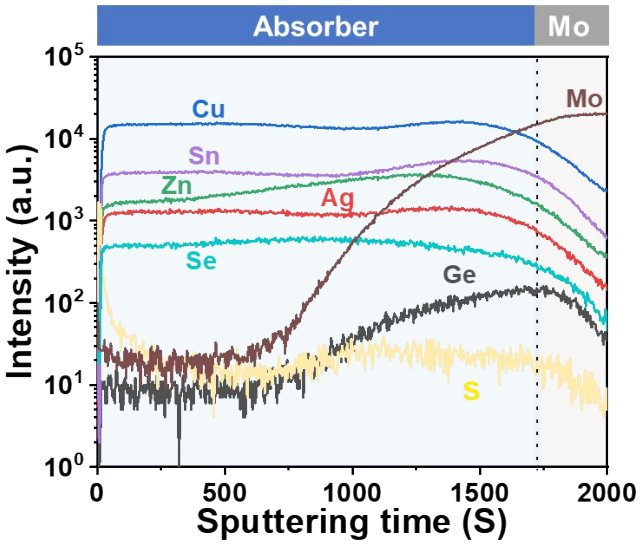

Figure S6. Elemental distribution profile of Ag and Ge along with constituent kesterite element in CZTSSe:Ag-Ge absorber layer.

Table S2. Comparison of relative defect density and estimated energy levels in reference, single and double cation incorporated CZTSSe samples.

Sample	Defect energy level (meV)	Defect density (cm^{-3})
Reference (CZTSSe)	198	5.21×10^{15}
Only Ag (Single cation)	86	2.0×10^{17}
Only Ge (Single cation)	126	4.0×10^{16}
Ag and Ge (Doble cation)	96	2.23×10^{15}

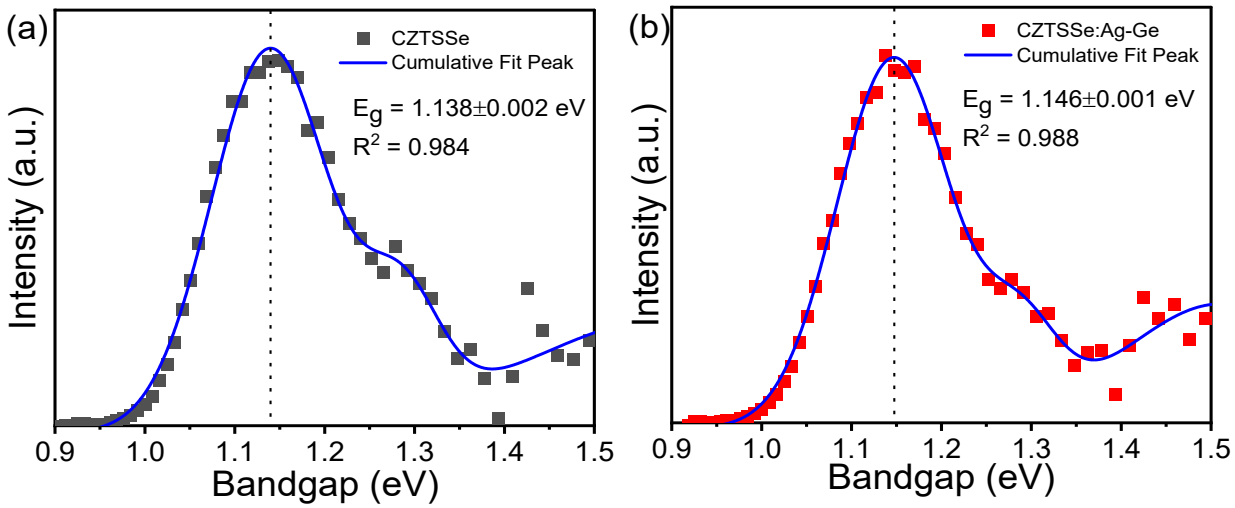

Figure S7. dEQE/dλ spectra for (a) CZTSSe and (b) CZTSSe: Ag-Ge devices, respectively.

Table S3. Light *J-V* and junction properties of the undoped CZTSSe and CZTSSe:Ag-Ge solar cells. The junction properties, device bandgap, and V_{oc}-deficit are estimated only for the most efficient device.

Sample code		V_{oc} (mV)	J_{sc} (mA/cm^2)	FF (%)	PCE (%)	R_s (Ω)	R_{sh} (Ω)	W_d (nm)	N_a (×10^{16} cm^{-3})	$E_{g\ (EQE)}$ (eV)	V_{oc}-deficit (mV)
CZTSSe	Avg	480 ±2.0	31.89 ±0.75	57 ±3	8.64 ±0.49	10.9 ±0.95	361 ±140	95	1.2	1.138 ±0.002	661
	Best	477	32.53	60	9.32	11.7	172				
CZTSSe : Ag-Ge	Avg	499 ±11	32.1 ±1.73	62 ±1	9.83 ±0.34	10.5 ±0.62	576 ±219	73	4.6	1.146 ±0.001	636
	Best	510	31.72	63	10.17	10.2	357				

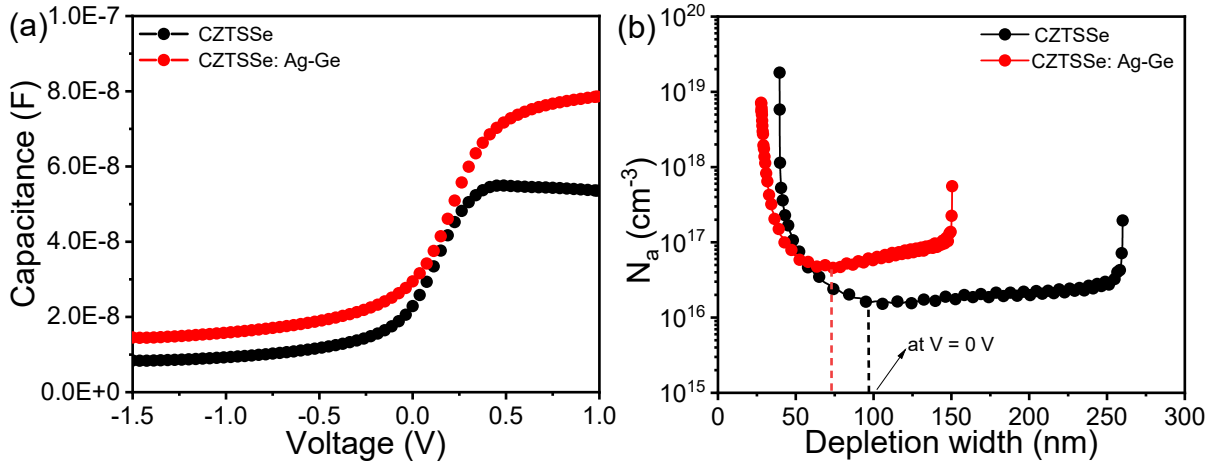

Figure S8. (a) Capacitance vs. voltage curve and (b) carrier concentration vs. depletion width for CZTSSe and CZTSSe: Ag-Ge devices.

Table S4. Detailed comparison among the different organic and inorganic IPV devices PCE and V_{oc} under indoor light conditions. (NA-Not available)

Material	IPV source	Light intensity (lux)	E_g (ev)	V_{oc} (mv)	J_{sc} (mA/cm^2)	FF (%)	Power output (μw/cm^2)	PCE (%)	Ref
CZTSSe	CFL	~700/400	1.3-1.4	~350/320	<0.1	~65	NA	~10/9	[S3]
CZTSSe	LED	~10000	NA	~250	<0.1	~56	NA	6%	[S4]

CZTS	Halogen lamp	400	1.5	395	0.15	30.9	19.10	NA	[S5]
CZTSe			1.0	173	0.52	25.2	23.70	NA	
CZTSSe			1.13	349	0.54	25.5	45.00	NA	
CZTSSe	WLED	1200	NA	200	0.26	31.0	16.16	NA	[S6]
CZTSSe:Ag			NA	310	0.29	44.0	39.57	NA	
CZTSSe:Ge			NA	280	0.25	42.0	29.73	NA	
CZTSSe	FL-4000 K	1200	NA	170	0.14	30.0	6.96	NA	
CZTSSe:Ag			NA	280	0.14	44.0	18.23	NA	
CZTSSe:Ge			NA	250	0.14	37.0	12.89	NA	
CZTSSe	WLED	1200	1.10	300	0.19	39.0	22.96	3.24	This work
	FL-4000K			300	0.17	38.0	16.19	3.95	
CZTSSe: Ag-Ge	WLED	1200	1.14	340	0.22	47.0	35.06	4.95	
	FL-4000K			360	0.13	50.0	23.99	5.85	
DSSC	CFL	200/1000		~520/610	NA	NA	6.6/37.9	NA	[S7]
a-Si		200/1000	1.6	~650/720	NA	NA	8.1/46.5	NA	
GaAs		200/1000	1.8-1.9	~800/900	NA	NA	13.8/80.5	NA	
GaInp		200/1000	1.8-1.9	~1100/1190	NA	NA	15.6/32.6	NA	
DSSC	LED	200/1000		~550/610	NA	NA	7.7/36.5	NA	
a-Si		200/1000	1.6	~680/720	NA	NA	9.4/46.4	NA	
GaAs		200/1000	1.8-1.9	~800/900	NA	NA	16.6/92.2	NA	
GaInp		200/1000	1.8-1.9	~1100/1180	NA	NA	17.6/87.2	NA	
CIGS	halogen lamp	1250	NA	NA	NA	NA	221	~4.4	[S8]
CIGS	FL-6500	2050	NA	NA	NA	NA	19	~2%	
CIGS	FL-4100	1850	NA	NA	NA	NA	23	~2.5	
CIGS	FL-3000	80	NA	NA	NA	NA	1	<1	
CIGS	UV	2380	NA	NA	NA	NA	19	~2	
c-Si	Halogen lamp	1250	NA	NA	NA	NA	295	~5.9	
c-Si	FL-6500	2050	NA	NA	NA	NA	55	~4.5	
c-Si	FL-4100	1850	NA	NA	NA	NA	71	~7	
c-Si	FL-3000	80	NA	NA	NA	NA	3	~3.5	
c-Si	UV	2380	NA	NA	NA	NA	44	~4.0	

The V_{oc} recovery was estimated using the following equation 1, 2, and 3, and calculated values are given in **Table S5**

$$Relative\ V_{oc}\ loss = \frac{\left(V_{oc\ (1\ sun)} - V_{oc\ (indoor\ condition)}\right)}{V_{oc\ (1\ sun)}} \quad \ldots\ldots(1)$$

$$V_{oc}\ loss\ (\%) = Relative\ V_{oc}\ loss \times 100\% \quad \ldots\ldots\ldots\ldots(2)$$

$$V_{oc}\ recovery\ (\%) = 100 - V_{oc}\ loss\ (\%) \quad \ldots\ldots\ (3)$$

Table S5. The V_{oc} recovery was calculated for best performing CZTSSe and CZTSSe:Ag-Ge devices under different light intensity conditions.

Device	Light source	Light intensity (lux)	1 Sun V_{oc} (mV)	Indoor V_{oc} (mV)	Relative V_{oc} loss	V_{oc} loss (%)	V_{oc} recovery (%)
CZTSSe	WLED	400	477	200	0.58	58.07	41.93
		800	477	280	0.41	41.30	58.70
		1200	477	300	0.37	37.11	62.89
	FL-4000K	400	477	170	0.64	64.36	35.64
		800	477	270	0.43	43.40	56.60
		1200	477	300	0.37	37.11	62.89
CZTSSe: Ag-Ge	WLED	400	510	290	0.43	43.14	56.86
		800	510	330	0.35	35.29	64.71
		1200	510	340	0.33	33.33	66.67
	FL-4000K	400	510	310	0.39	39.22	60.78
		800	510	340	0.33	33.33	66.67
		1200	510	360	0.29	29.41	70.59

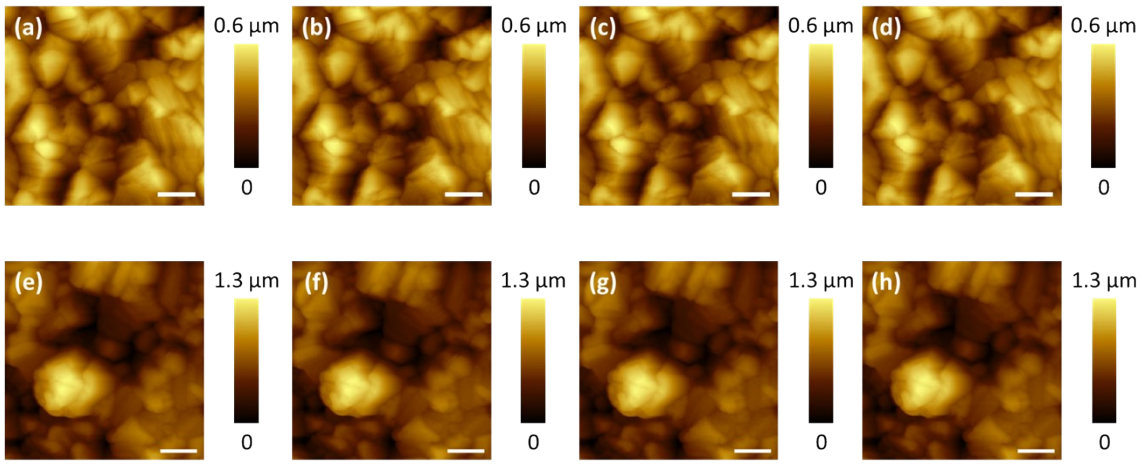

Figure S9. Topography images of (a) CZTSSe and (b) CZTSSe: Ag-Ge in dark, (c-d) under 400 lux, (e-f) under 800 lux, (g-h) under 1200 lux.

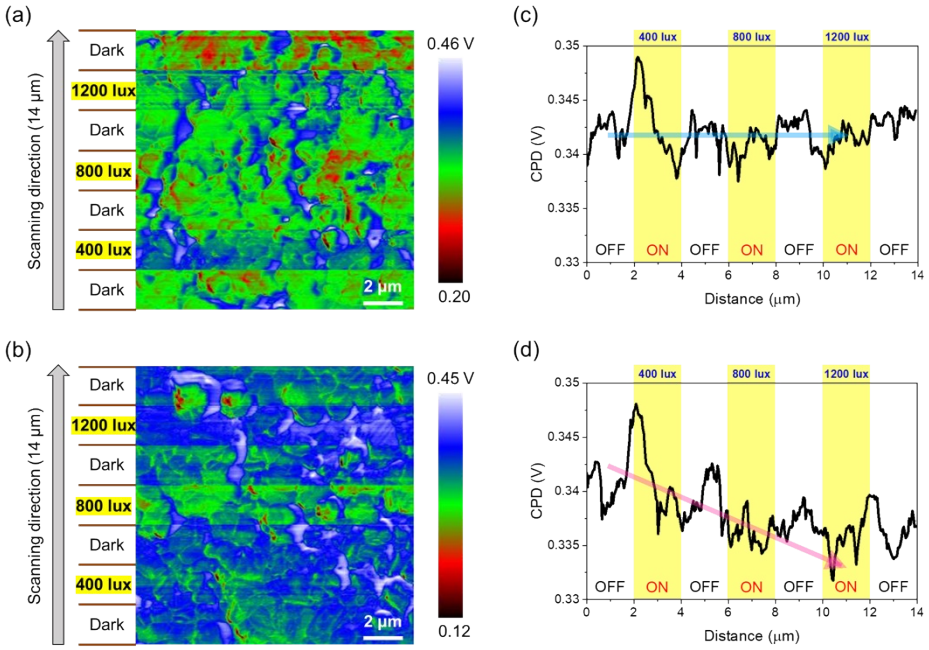

Figure S10. CPD maps of (a) CZTSSe and (b) CZTSSe: Ag-Ge samples were obtained by illumination on and off measurements (Dark – 400 lux – Dark – 800 lux – Dark – 1200 lux – Dark). (c)-(d) Average CPD line profiles of CZTSSe and CZTSSe: Ag-Ge, respectively, obtained from corresponding CPD maps from (a)-(b).

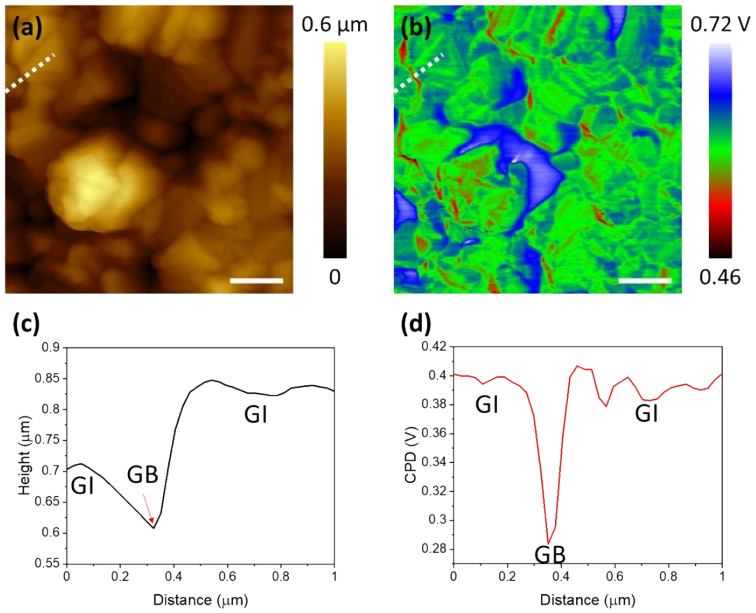

Figure S11. Example of obtaining the CPD value at grain interiors (GIs) and grain boundaries (GBs). (a) Topography, (b) CPD map of CZTSSe:Ag-Ge sample under dark condition, (c) line profile of height obtained from white dotted line in (a), and (d) line profile of CPD obtained from white dotted line in (b).

References

[S1] K. S. Gour, V. C. Karade, M. Lee, J. S. Jang, E. Jo, P. Babar, H. Shim, J. S. Yun, J. Park, J. H. Kim, ACS Appl. Energy Mater. 2022, 5, 2024.

[S2] M. G. Gang, V. C. Karade, M. P. Suryawanshi, H. Yoo, M. He, X. Hao, I. J. Lee, B. H. Lee, S. W. Shin, J. H. Kim, ACS Appl. Mater. Interfaces 2021, 13, 3959.

[S3] P. D. Antunez, D. M. Bishop, Y. Luo, R. Haight, Nat. Energy 2017, 2, 884.

[S4] H. Deng, Q. Sun, Z. Yang, W. Li, Q. Yan, C. Zhang, Q. Zheng, X. Wang, Y. Lai, S. Cheng, Nat. Commun. 2021, 12, 1.

[S5] J. Park, H. Yoo, V. Karade, K. S. Gour, E. Choi, M. Kim, X. Hao, S. J. Shin, J. Kim, H. Shim, D. Kim, J. Kim, J. Yun, J. H. Kim, J. Mater. Chem. A 2020, 8, 14538.

[S6] J. Park, M. Lee, V. Karade, S. J. Shin, H. Yoo, H. Shim, K. S. Gour, D. Kim, J. Hwang, D. Shin, J. Seidel, J. H. Kim, J. Yun, J. H. Kim, Sol. RRL 2021, 5, 2100020.

[S7] I. Mathews, P. J. King, F. Stafford, R. Frizzell, IEEE J. Photovoltaics 2016, 6, 230.

[S8] C. Yang, R. P. Xue, X. Li, X. Q. Zhang, Z. Y. Wu, Renew. Energy 2020, 161, 836.